A selective photoaffinity probe that enables assessment of cannabinoid CB2 receptor expression and ligand engagement in human cells

Soethoudt, M.; Stolze, S.C.; Westphal, M.V.; Stralen, L. van; Martella, A.; Rooden, E.J. van; ... ; Stelt, M. van der

JACS JOURNAL OF THE AMERICAN CHEMICAL SOCIETY
Article
Cite This: J. Am. Chem. Soc. XXXX, XXX, XXX−XXX
pubs.acs.org/JACS

Selective Photoaffinity Probe That Enables Assessment of Cannabinoid CB_2 Receptor Expression and Ligand Engagement in Human Cells

Marjolein Soethoudt,[†,‡] Sara C. Stolze,[§,■] Matthias V. Westphal,[∥] Luuk van Stralen,[⊥] Andrea Martella,[†] Eva J. van Rooden,[†] Wolfgang Guba,[#] Zoltan V. Varga,[▽] Hui Deng,[†,○] Sander I. van Kasteren,[§] Uwe Grether,[#] Adriaan P. IJzerman,[‡] Pal Pacher,[▽] Erick M. Carreira,[∥] Herman S. Overkleeft,[§] Andreea Ioan-Facsinay,[⊥] Laura H. Heitman,[‡] and Mario van der Stelt*[,†]

[†]Department of Molecular Physiology, Leiden Institute of Chemistry, [‡]Research Division of Drug Discovery and Safety, Leiden Academic Centre for Drug Research, and [§]Bio-Organic Synthesis, Leiden Institute of Chemistry, Leiden University, Einsteinweg 55, Leiden 2333 CC, The Netherlands

[∥]Laboratorium für Organische Chemie, Eidgenössische Technische Hochschule Zürich, Vladimir-Prelog-Weg 3, Zürich 8093, Switzerland

[⊥]Department of Rheumatology, Leiden University Medical Center, Albinusdreef 2, Leiden 2333 ZA, The Netherlands

[#]Roche Innovation Center Basel, F. Hoffmann-La Roche Ltd., Grenzacherstrasse 124, Basel 4070, Switzerland

[▽]Laboratory of Cardiovascular Physiology and Tissue Injury, National Institute on Alcohol Abuse and Alcoholism, National Institutes of Health, 5625 Fishers Lane, Rockville, Maryland 20852, United States

Supporting Information

ABSTRACT: Chemical tools and methods that report on G protein-coupled receptor (GPCR) expression levels and receptor occupancy by small molecules are highly desirable. We report the development of LEI121 as a photoreactive probe to study the type 2 cannabinoid receptor (CB_2R), a promising GPCR to treat tissue injury and inflammatory diseases. LEI121 is the first CB_2R-selective bifunctional probe that covalently captures CB_2R upon photoactivation. An incorporated alkyne serves as ligation handle for the introduction of reporter groups. LEI121 enables target engagement studies and visualization of endogenously expressed CB_2R in HL-60 as well as primary human immune cells using flow cytometry. Our findings show that strategically functionalized probes allow monitoring of endogenous GPCR expression and engagement in human cells using tandem photoclick chemistry and hold promise as biomarkers in translational drug discovery.

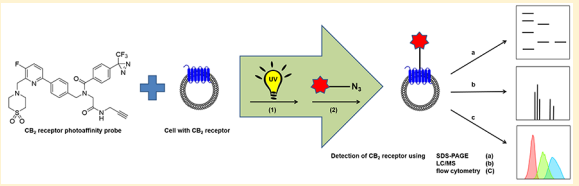

INTRODUCTION

The G protein-coupled receptors (GPCR) comprise a 700-membered family of seven-transmembrane domain proteins expressed at the cell membrane.[1,2] They convey extracellular signals from different types of stimuli, such as light, (peptide) hormones, and neurotransmitters, to intracellular second messenger systems, thereby allowing cells to respond to their environment. GPCRs are involved in the regulation of many physiological processes, including vision, behavior, mood, energy balance, immunity, and inflammation.[3] GPCRs are also an important class of drug targets and offer great potential for the discovery of new therapeutics for a variety of diseases.[1] The type 2 cannabinoid receptor (CB_2R),[4] subject of the here-presented study, is a promising GPCR for the treatment of tissue injury and inflammatory diseases.[5,6]

The CB_2R plays an important role in cell migration and immunosuppression. It shares extensive sequence homology with the type 1 cannabinoid receptor (CB_1R, 44% overall homology, and 68% homology in the ligand-binding domain),[4] which is highly expressed in the central nervous system.[7] Both CB_1R and CB_2R are activated by Δ^9-tetrahydrocannabinol (Δ^9-THC, Figure S1), the main psychoactive constituent of marijuana.[8] CB_2R is predominantly found in cells of the immune system and is upregulated during various pathophysiological conditions.[5,9] Selective activation of the CB_2R may confer therapeutic benefits without inducing adverse side effects associated with CB_1R modulation.[10] This spurred drug discovery efforts by academic groups and the pharmaceutical industry resulting in the identification of highly selective CB_2R agonists, such as LEI101, HU308, and HU910 (for structures, see Figure S1).[11−14] These CB_2R agonists show robust efficacy in various animal models of chronic and inflammatory pain, diabetic neuro- and nephropathy, liver cirrhosis, and ischemic-reperfusion injury.[11−14]

The successful development of new drugs strongly depends on our understanding of their underlying molecular and cellular mechanism of action.[15,16] An important step that drives the

Received: October 23, 2017
Published: February 8, 2018

DOI: 10.1021/jacs.7b11281
J. Am. Chem. Soc. XXXX, XXX, XXX−XXX

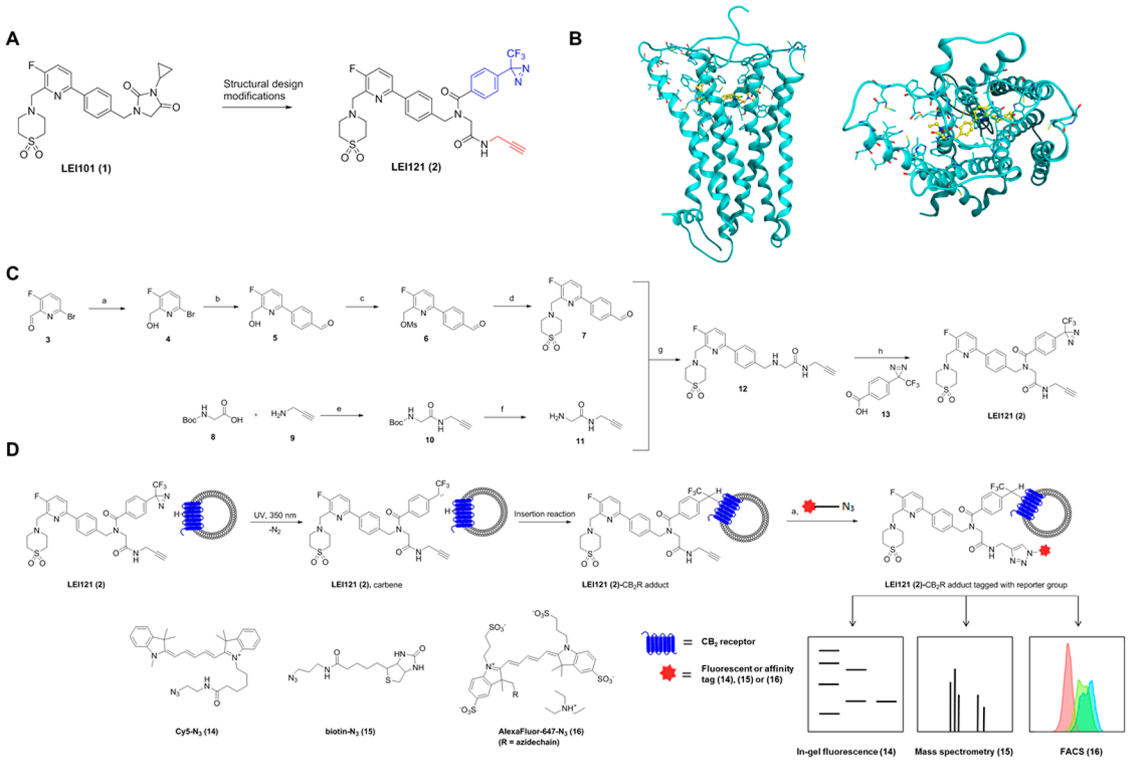

Figure 1. Design, synthesis, and two-step photoaffinity labeling of LEI121. (A) LEI121 was designed by replacing the hydantoin group of LEI101 by a central amide that carries both the photoreactive diazirine moiety (blue) and the ligation handle (red). (B) LEI101 was docked into a CB_2R homology model based on a recently published CB_1R crystal structure.[42] (C) Synthesis of LEI121, reagents and conditions: (a) $NaBH_4$, DCM:MeOH (2:1), rt, 99%; (b) (4-formylphenyl)boronic acid, $Pd(PPh_3)_4$, K_2CO_3, toluene:EtOH (4:1), 80 °C, 89%; (c) DiPEA, Ms-Cl, DCM, 0 °C, quant.; (d) thiomorpholine 1,1-dioxide, K_2CO_3, ACN, 60 °C, 95%; (e) *N*-methylmorpholine, HOBt, EDC, DCM, quant.; (f) HCl, dioxane, 60%; (g) K_2CO_3, $NaBH(OAc)_3$, MeOH:DCM (1:1), 28%; and (h) diazirine **13**, EDC, HOBt, DCM, 14%. (D) Two-step photoaffinity labeling. After incubation of proteome or whole cells with the probe, UV-irradiation causes the formation of a carbene, which is able to insert itself into a C−H, O−H, or N−H bond of the targeted protein. The resulting protein−probe complex is tagged using a copper-catalyzed azide−alkyne cycloaddition (CuAAC) with the following conditions: NaAsc, $CuSO_4$, THPTA, and tag **14**, **15**, or **16** to enable SDS-PAGE, mass spectrometry, or flow cytometry analysis, respectively.

drug discovery processes is the determination of the cellular expression profile of the target protein in humans.[17] This provides a challenge for the study of GPCRs, because they are usually expressed at very low levels in native cells and tissues.[18] In addition, GPCRs are known for their inducible nature, which includes the adaptation from inactive to active conformations and internalization and desensitization upon durable activation. These factors may lead to variable surface expression of the GPCRs. Antibodies can be used to detect surface expression of GPCRs, but specific antibodies against CB_2R are currently lacking, which hampers the detection of CB_2R by standard biochemical methods.[18−20]

Another important aspect in drug development is to verify that the drug candidate fully engages with its intended target in vivo.[15] Information on target engagement at a certain concentration will help to select the best compound as a drug candidate and may guide the dose selection by providing information on full target engagement, while minimizing the risk for untoward off-target interactions by preventing over-exposure. Currently, there are no biomarkers for target occupancy of CB_2R available, complicating the translation of preclinical data and dose selection of CB_2R agonists in the clinic.[12,21]

Chemical probes are highly useful tools to map ligand−protein interactions in living systems.[17] Positron emission tomography (PET) tracers, for instance, are widely applied to determine receptor occupancy of drug candidates in patients. However, the disadvantages of such probes are that they require a facility for radiolabeling and have limited cellular resolution.

Fluorescent and biotinylated probes are also used to study GPCR function,[22−30] but the size of the reporter group may interfere with receptor affinity and/or selectivity,[22,23,25,26] may increase nonspecific binding,[23,26,27] and may lead to a decrease in metabolic stability.[22] Another drawback is that such probes rely on noncovalent interactions with the receptor, which can be easily disrupted by various experimental conditions. The latter can be avoided by using photoaffinity probes that employ a light-responsive element to covalently cross-link the compound with its target protein upon irradiation.[31−34] Photoreactive probes have been previously used to map GPCR binding sites and ligand−receptor interactions with or without the use of radioactive isotopes for detection,[34−36] and to capture the receptor in heterologous overexpression systems,[37] but not for GPCR target engagement in endogenous expressing systems. To circumvent the problems associated with large reporter groups or radioactive isotopes,[35,36] photoaffinity probes, containing a strategic ligation handle (e.g., alkyne or azide), to introduce a fluorescent or affinity tag (e.g., biotin) after cross-linking to a protein, have emerged as powerful tools to visualize small molecule−protein interactions in living systems.[15,38−40] This strategy is known as two-step photoaffinity-based protein profiling (pAfBPP).[31]

DOI: 10.1021/jacs.7b11281
J. Am. Chem. Soc. XXXX, XXX, XXX−XXX

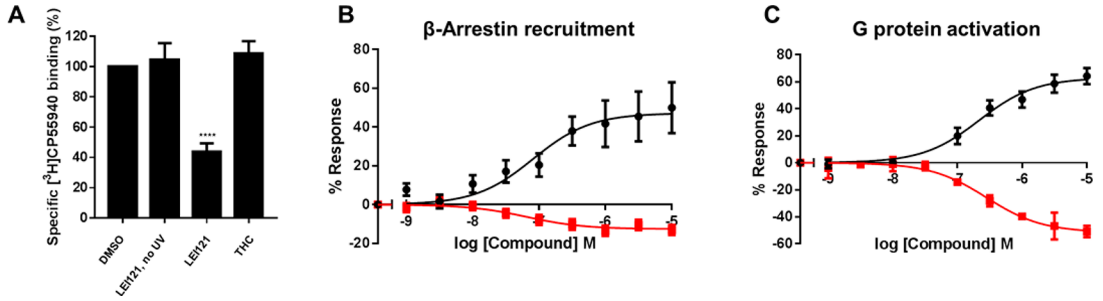

Figure 2. Molecular pharmacology of LEI101 versus LEI121. (A) Reduced [^{3}H]CP55940 binding to CB_2R in LEI121-treated membranes from CB_2R-overexpressing CHO cells was observed after UV-irradiation and washout, but not in THC- or nonirradiated LEI121-treated membranes. Data presented are the mean ± SEM of three (two in case of THC) independent experiments performed in duplicate. Statistics performed is a two-tailed *t*-test (****p-value < 0.0001). (B,C) β-Arrestin recruitment and G protein activation were measured as described previously,[12,47] showing inverse agonistic activity of LEI121 (■) (β-arrestin recruitment pEC_{50} (E_{max}), 7.3 ± 0.3 (−12 ± 4); G protein activation pEC_{50} (E_{max}), 6.6 ± 0.2 (−50 ± 7)), which is in contrast to the agonism activity of LEI101 (●)[11] (β-arrestin recruitment pEC_{50} (E_{max}), 7.0 ± 0.3 (41 ± 6); G protein activation pEC_{50} (E_{max}), 6.6 ± 0.2 (65 ± 8)). Efficacy (E_{max}) is normalized to the effect of 10 μM CP55940. Data are presented as the mean ± SEM of three independent experiments performed in duplicate, except for β-arrestin recruitment of LEI121 (4 experiments in duplicate).

Inspired by these established and emerging concepts, we describe herein a two-step pA*f*BPP strategy to visualize endogenous CB_2R expression and target engagement in primary human cells. To the best of our knowledge, this is the first report of a two-step photoaffinity probe being used for such studies on a GPCR. Photoaffinity probe LEI121 contains a photoactivatable diazirine group, enabling CB_2R cross-linking upon UV-irradiation and an alkyne moiety for bio-orthogonal conjugation to various reporter groups. LEI121 enabled target engagement studies and visualization of CB_2R on HL-60 cells and primary human immune cells. Our results show that strategically functionalized photoreactive probes can monitor endogenous GPCR expression and ligand engagement. Such probes hold promise as biomarkers for target engagement studies in translational drug discovery.

RESULTS

Design and Synthesis of LEI121. The ideal bio-orthogonal photoaffinity probes are normally composed of three distinct features:[31] (1) a recognition element that binds to the intended target in a potent and selective manner, (2) a photoactivatable group, which, upon irradiation, forms a reactive intermediate capable of covalently binding the target protein, but is otherwise stable in the absence of the external activating signal, and (3) a ligation handle that can be used to couple the probe to different reporter tags using bio-orthogonal chemistry. The latter two functionalities should be small and properly positioned to minimally affect the probe's binding affinity for the target or the selectivity of the probe. In addition, the probe should have favorable physicochemical properties, displaying aqueous solubility with a minimum of nonspecific interactions. In view of the stringent set of criteria, we choose 3-cyclopropyl-1-(4-(6-((1,1-dioxidothiomorpholino)methyl)-5-fluoropyridin-2-yl)benzyl)imida-zoleidine-2,4-dione (LEI101, **1**, Figure 1A) as our starting point to develop a new photoaffinity probe for the CB_2R. LEI101 is a highly selective CB_2R agonist with favorable physicochemical properties, such as low molecular weight (MW 473 Da), low lipophilicity (cLogP 1.0), and high solubility (89 mg/L).[11] LEI101 has oral efficacy in a neuropathic pain model and in a clinically relevant murine model of nephropathy in a CB_2R-dependent manner.[11]

To identify appropriate positions in the scaffold of LEI101 for the introduction of the two key elements, a photoreactive group and ligation handle, we conducted a careful analysis involving the available structure−activity relationship (SAR) data previously reported for LEI101.[41] Furthermore, we performed a docking study of LEI101 with a homology model of the human CB_2R (hCB_2R), based on a recently published crystal structure of the hCB_1R in complex with the antagonist AM6538 (Figure 1B).[42] We surmised that opening the hydantoin moiety would enable the introduction of exit-vectors incorporating functional groups to introduce a photoreactive group and a ligation handle. We selected trifluoromethyl-diazirine-benzoyl as a relatively small photoreactive group and a propargyl substituent as ligation handle. Combining these functional groups with the biaryl scaffold of LEI101 led to the design of the CB_2R selective photoaffinity probe LEI121 (**2**) (Figure 1A).

The synthesis of LEI121 commenced with reduction of commercially available aldehyde **3**, followed by Suzuki coupling with 4-formylboronic acid to afford intermediate **5**, which was converted into compound **7** via mesylation and nucleophilic substitution. Building block **11** was synthesized in two steps from Boc-protected glycine **8** following literature procedures.[43]

Probe precursor **12** was obtained via reductive amination of aldehyde **7** using building block **11**. Peptide coupling of amine **12** with commercially available diazirine **13** furnished LEI121 (Figure 1C). Figure 1D shows the two-step photoaffinity labeling workflow with LEI121: after covalent CB_2R adduct formation by insertion of a reactive carbene, generated upon photoactivation of LEI121 (irradiation at 350 nm), ligation of CY5-N_3 (**14**), biotin-N_3 (**15**), or AlexaFluor-647-N_3 (**16**) is effected by Cu(I)-catalyzed azide−alkyne cycloaddition (CuAAC, "click"-reaction).[44,45] The conjugated constructs enable subsequent visualization by in-gel fluorescence imaging after electrophoresis on polyacrylamide (SDS-PAGE), mass spectrometry, and FACS analysis, respectively.

Molecular Pharmacology of LEI121 on Human CB_2 and CB_1 Receptors. We first determined the affinity of LEI121 (without UV-irradiation) for the hCB_2R in a radioligand binding competition assay employing [^{3}H]-CP55940 (a tritiated high affinity ligand for CB_2R) using membranes derived from recombinant hCB_2R-overexpressing Chinese hamster ovary (CHO) cells (CB_2R-CHO cells), as described previously.[12] LEI121 displaced [^{3}H]-CP55940 in a concentration-dependent manner (pK_i = 7.2 ± 0.4), similarly to LEI101 (pK_i = 7.5 ± 0.1) (Table S1).[11] Importantly, LEI121 did not show any affinity (pK_i < 5) for hCB_1R in a similar

DOI: 10.1021/jacs.7b11281
J. Am. Chem. Soc. XXXX, XXX, XXX−XXX

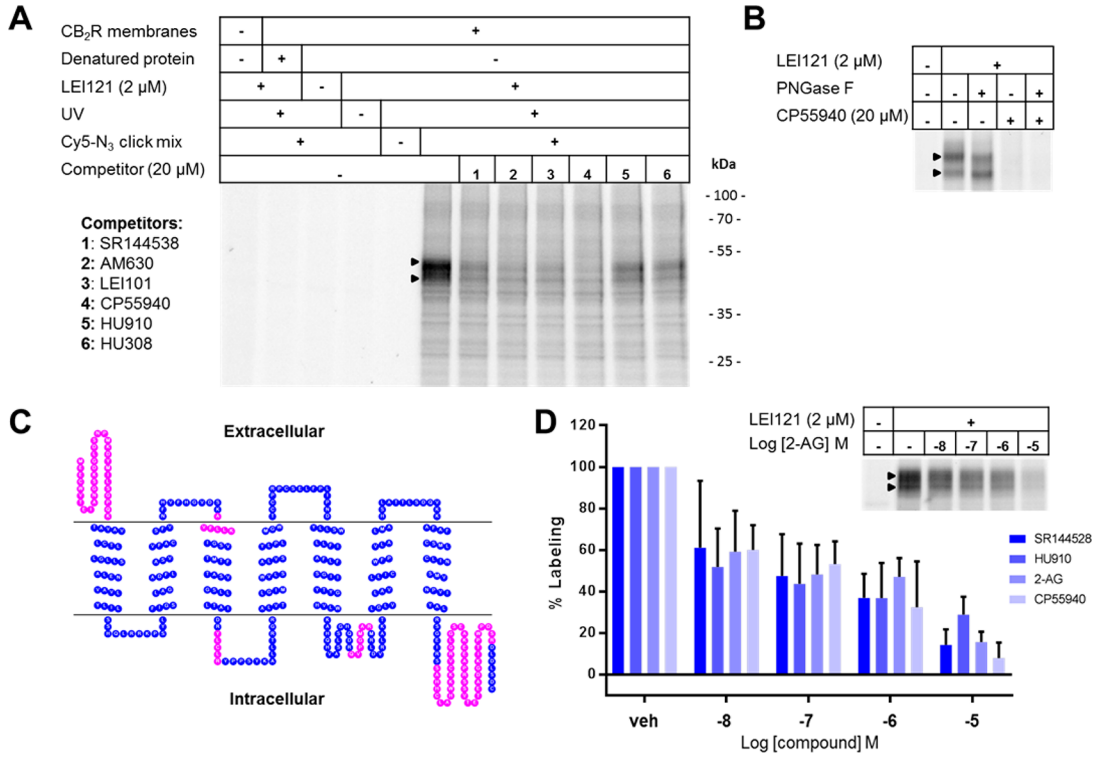

Figure 3. Validation of CB_2R labeling by LEI121 in CB_2R-overexpressing CHO cells. (A) LEI121 labels displaceable bands (▶ = CB_2R) specifically in CB_2R-overexpressing membranes, not in wild-type CHO membranes, and only in the presence of all necessary components (active protein, probe, UV-irradiation, ligation components). (B) Addition of PNGase F shows a decrease of higher MW glycosylated CB_2R bands, and an increase in full-length, probe-bound CB_2R signal (~41 kDa). The gel shown is a representative result of three independent experiments. (C) Isolation of CB_2R was achieved in live CB_2R-overexpressing cells by ligation with biotin-N_3 (**15**), followed by avidin enrichment, trypsinization, and proteomics. CB_2R peptides identified from three independent experiments are highlighted in magenta. (D) Quantification of dose-dependent displacement of LEI121-labeled bands in SDS-PAGE experiments by different cannabinoid ligands. Results shown are the mean ± SEM of 2 (CP55940 and 2-AG) or 3 (SR144528 and HU910) independent experiments. The inlay shown is a representative gel of concentration-dependent displacement of LEI121 labeling by 2-AG (see also Figure S8).

competition assay (Table S1).[12] Next, we tested whether UV-irradiation would result in covalent binding of LEI121 to CB_2R. Indeed, specific binding of [^{3}H]-CP55940 to hCB_2R membranes was significantly reduced in samples pretreated with LEI121 and cross-linked by UV-irradiation (λ = 350 nm, 5 min), using a CaproBox,[46] a device used for controlled irradiation of biological samples with simultaneous cooling at 4 °C, to counteract the heat induced by the irradiation. Specific binding of [^{3}H]-CP55940 remained unchanged when the irradiation step was omitted or the nonphotoreactive ligand Δ^9-THC was used (Figure 2A). These findings indicate that LEI121 undergoes covalent and irreversible cross-linking to the CB_2R binding site upon UV-irradiation.

Because CB_2R ligands can modulate different intracellular signal transduction pathways, we determined the potency of LEI121 in two functional assays by measuring β-arrestin recruitment and G protein activation.[12,47]

As previously reported, LEI101 behaved as partial agonist in both assays (Figure 2B,C and Table S1).[11] LEI121 did not activate either of the two pathways, but was able to reduce the constitutive activity of the receptor, thereby classifying as an inverse agonist (see Figure 2B,C and Table S1). Although the exact reason for the switch in functional activity between LEI101 and LEI121 is currently unknown, it is well-known that structural changes within a chemical series may result in a reversal of functional activity (Figure S2).[48]

Visualization of CB_2 Receptors by LEI121 Using Affinity-Based Protein Profiling. LEI121 was tested for its ability to visualize CB_2R by two-step p*Af*BPP. To this end, membrane preparations of hCB_2R-overexpressing CHO cells were incubated with LEI121. Cross-linking was again effected by UV-irradiation (λ = 350 nm). Next, the membranes were subjected to copper(I)-catalyzed click reaction conditions, utilizing Cy5-N_3 (**14**) as the fluorescent azide to analyze the probe–protein complex by SDS-PAGE and in-gel fluorescence imaging. In this manner, two major bands with an apparent molecular weight of ~47 and ~41 kDa (Figure 3A) were visualized, and these were absent in membranes from wild-type CHO cells treated in the same manner. Heat-induced denaturation prior to probe incubation also resulted in a loss of fluorescent bands, indicating that the recognition is dependent on an intact three-dimensional protein conformation. The bands were also absent in non-UV treated samples, demonstrating that the probe does not covalently interact with CB_2Rs in the absence of irradiation. Furthermore, omission of the click-mixture showed that labeling was dependent on copper(I)-catalyzed azide alkyne click ligation (Figure 3A). CB_2R has a glycosylation site on its N-terminus,[49] and a glycosylated form of CB_2R (~46 kDa) has previously been reported.[50] Therefore, we wondered whether the two fluorescent bands could reflect different glycosylation forms. We treated the membranes with a glycosidase (PNGaseF) to remove *N*-linked glycans. This resulted in decreased

DOI: 10.1021/jacs.7b11281
J. Am. Chem. Soc. XXXX, XXX, XXX−XXX

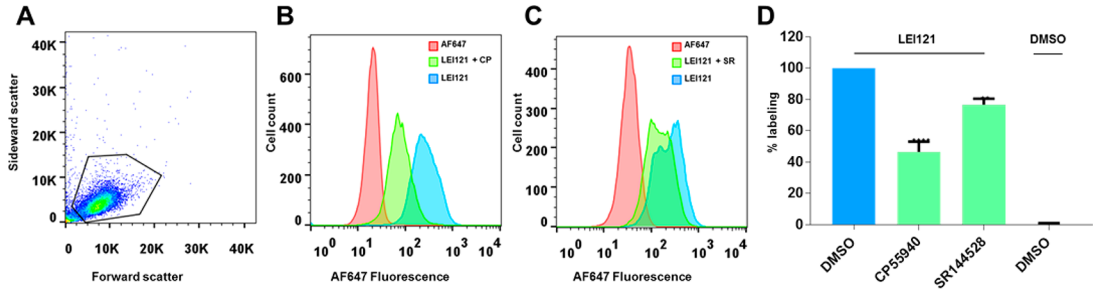

Figure 4. Visualization of endogenous CB_2R expression in live HL-60 cells by LEI121. (A) Representative dot plot of the selected HL-60 cell population for each individual experiment. (B,C) Representative histograms showing fluorescence intensity differences between the untreated sample (AF647-fluorophore only), the LEI121-treated sample, and the sample with CP55940 (CP, B) or SR144528 (SR, C). (D) Pretreatment with CP55940 (10 μM) and SR144528 (20 μM) induced ~50% and ~25% displacement, respectively, of the labeling induced by LEI121. Statistics performed was a two-tailed *t*-test, and the results shown are the mean ± SEM of the background-corrected, normalized mean fluorescence intensity (MFI) values of three independent experiments performed in duplicate (**p-value < 0.01, ****p-value < 0.0001).

fluorescence of the 47 kDa band, while the fluorescence intensity of the 41 kDa band, which corresponds to the molecular weight of the CB_2R-probe-Cy5 adduct, increased (Figure 3b). Of note, longer incubation times or higher amounts of PNGaseF resulted in a loss of signal, which might reflect protein precipitation due to loss of protein solubility. In-gel digestion and mass spectrometry analysis identified CB_2R peptides in both bands (Table S2). Taken together, these results could suggest that the high-MW labeled bands represent glycosylated forms of the receptor, although other post-translational modifications may also be present on the CB_2R. Next, we validated that the band intensity was dependent on probe and protein concentration (Figure S3). With the total amount of CB_2R (B_{max}) for the membrane preparations of this cell line set at around ~15 pmol/mg protein (as determined by radioligand saturation studies), we calculated the detection limit of the probe to be around 9 fmol of CB_2R protein. Of note, labeling of CB_2R, albeit less intense, could also be obtained with two other photoaffinity probes, behaving as CB_2R agonists: LEI120, a close analogue of LEI121, and RO7239315, which has a completely different chemotype that is based on the structure of HU308 (Supporting Information Figures 4 and 5, respectively).[14] Interestingly, LEI120 and three analogues of RO7239315 showed less labeling (Supporting Information Figures 4 and 5), respectively. This indicated that a subtle change in positioning of the diazirine of the probes in the binding site plays an important role in the labeling efficiency. It is hypothesized that the switch in functional behavior of LEI121 and LEI120 is associated with the basic tertiary amine in LEI120, whereas the corresponding nitrogen in LEI121 is a tertiary amide without hydrogen-bonding acceptor or donor properties.

The CB_2R binding cavity is not favorable for charged interactions around the position of the nitrogen. Therefore, LEI121 has more favorable interactions than LEI120 with the receptor, which might explain its higher labeling efficiency.

To unequivocally prove that CB_2R is captured by LEI121, we incubated live human CB_2R-overexpressing CHO cells with LEI121. Subsequent UV-irradiation and ligation with biotin-N_3 (**15**) for affinity enrichment on avidin agarose beads enabled receptor identification by mass spectrometry-based proteomics. In three independent experiments, we identified CB_2R-specific peptides that belonged to the extra- and intracellular regions of the receptor (Figure 3C, Table S3). The identified CB_2R peptides were absent in samples from wild-type CHO cells and nonirradiated samples. CHO-CB_2R cells pretreated with CP55940 revealed a 78 ± 6% inhibition of CB_2R target engagement by LEI121 (Figure S6a,b).

Taken together, these results show that LEI121 is able to capture the hCB_2R using tandem photoclick chemistry. Of note, five other proteins were identified as potential off-targets of LEI121, that is, multidrug resistance protein 1, protein disulfide isomerase, mitochondrial carnitine/acylcarnitine carrier protein, glutathione *S*-transferase Mu 6, and 26S proteasome non-ATPase regulatory subunit 3 (Figure S7). CP55940 only reduced the abundance of CB_2R (Figure S6c), which indicates that the displaceable signal by CP55940 is CB_2R-specific.

Next, we explored whether the probe could be used in a competition format to test target engagement of various ligands representing distinct chemical classes and exhibiting different functional activities. Highly selective CB_2R agonists (LEI101, HU910, and HU308), CB_2R inverse agonists (SR144528 and AM630), CBR agonist CP55940, and the endocannabinoid 2-arachidonoylglycerol (2-AG) (for structures, see Figure S1) all prevented labeling of both bands by LEI121 (Figure 3A,D). Concentration-dependent displacement was observed for SR144528, HU910, 2-AG, and CP55940 (Figure S8). CP55940, the most potent CB_2R ligand in the series, showed the strongest reduction in CB_2R labeling by LEI121 (Figure 3A; Figure S8). Of note, LEI121 was not able to label CB_1R in a similar experiment using membranes of CB_1R-overexpressing CHO cells (Figure S9). Collectively, the results showed that LEI121 is able to capture and visualize the human CB_2R and its ligand engagement in heterologous overexpression systems.

Visualization and Target Engagement of Endogenous CB_2R in Human Cells. To test the ability of LEI121 to visualize endogenous CB_2R expression in live human cells, we used the human promyelocytic leukemia cell line HL-60, a fast-growing cell line widely used to study endogenously expressed CB_2R.[9,51,52] Because CB_2R expression in these cells was too low to reveal a specific CB_2R band using gel-based fluorescence imaging, we turned to fluorescence-activated cell sorting (FACS), a specialized form of flow cytometry. AlexaFluor-647-N_3 (**16**) was preferred over the Cy5 dye (**14**) due to the lower background fluorescence in FACS analysis. Incubation of HL-60 cells with LEI121 followed by tandem photoclick chemistry resulted in a population of cells that demonstrated increased fluorescence (Figure 4). Preincubation with CP55940 or SR144528 showed significant reductions in mean fluorescence intensity, thereby indicating that CB_2R was

DOI: 10.1021/jacs.7b11281
J. Am. Chem. Soc. XXXX, XXX, XXX−XXX

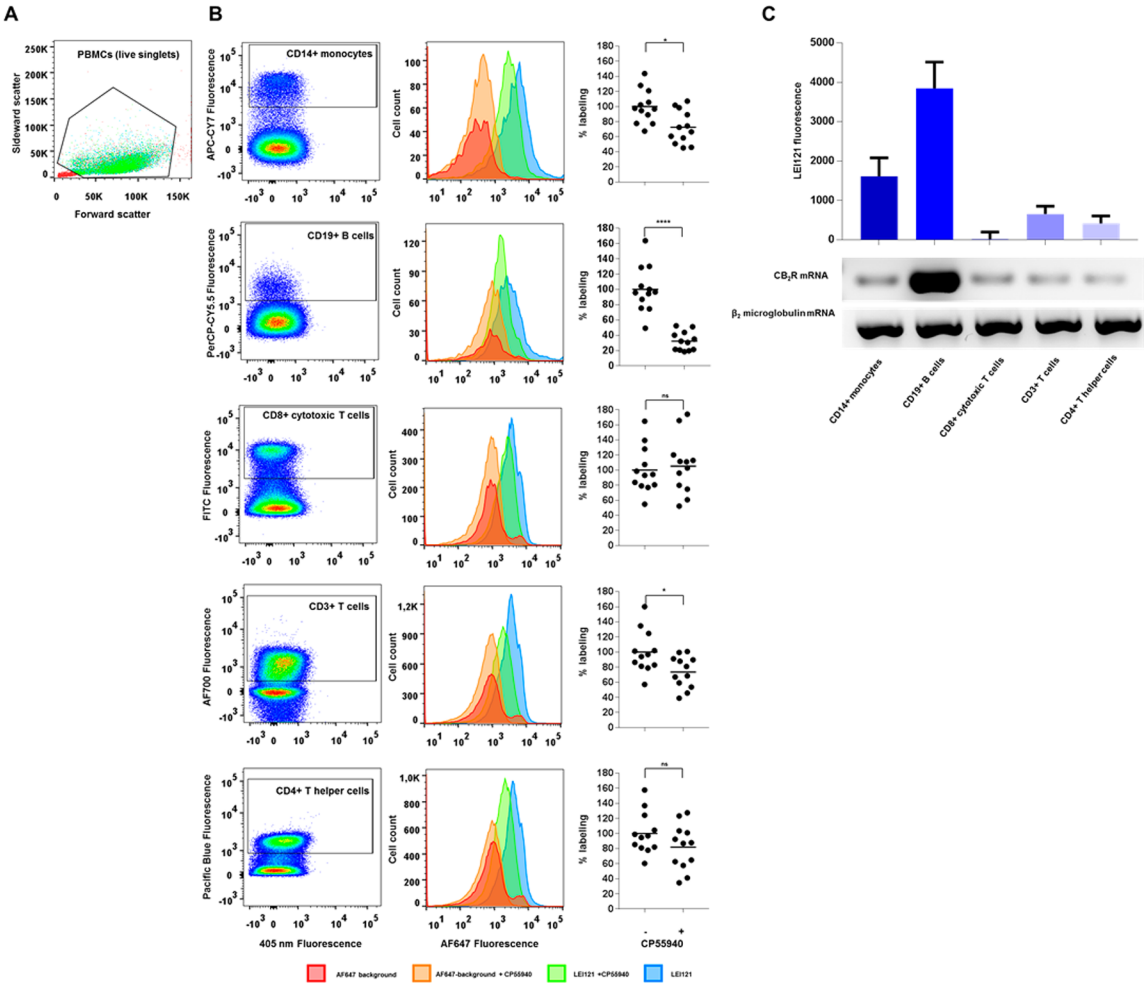

Figure 5. Visualization of endogenous CB_2R expression in PBMCs by LEI121. (A) Representative dot plot of the selected PBMC population (debris, doublets, and dead cells excluded). (B) From left to right: representative dot plots of selected positive populations, representative histograms of these populations to show fluorescence intensity differences, and scatter plots showing % labeling by LEI121 ∓ CP55940 of four donors, in triplicate (n = 12), normalized to the average maximum LEI121 signal per donor. The line represents the mean. Statistics was performed using a two-tailed t-test (*p-value < 0.05, ****p-value < 0.0001, ns = not significant) on the mean background-corrected, normalized MFI values of LEI121 ∓ CP55940 (N = 4). Significant displacement with CP55940 was observed in $CD3^+$ T cells, $CD14^+$ monocytes, and $CD19^+$ B cells. (C) The specific fluorescent signal of LEI121 indicates the level of CB_2R expression in these cell types. The highest signal was found in $CD19^+$ B cells, which is also the case for the level of CB_2R mRNA expression measured for these cell types. The β_2 microglobulin mRNA expression per cell type was determined as control. Bar graph shows the mean ± SEM of background-corrected specific fluorescence of LEI121 (for details of the calculations in (B) and (C), see Table S3 and Data Analysis).

successfully engaged by these ligands (Figure 4), as CB_2R is the only shared protein target of these molecules (Figure S6).

Finally, we assessed the ability of LEI121 to visualize endogenous CB_2R expression in primary human cells. To this end, peripheral blood mononuclear cells (PBMCs) from four healthy donors were isolated. PBMCs contain different immune cell subtypes that can be distinguished on the basis of the expression of specific cell surface markers using a panel of fluorescently labeled antibodies. For example, antibodies against Cluster of Differentiation 3 (CD3) detect the total T-cell population, whereas T-helper cells and cytotoxic T-cells are recognized by antibodies against CD4 and CD8, respectively. The B lymphocytes are targeted by antibodies against CD19 and monocytes by antibodies against CD14.[53] To assess which specific cell population expresses CB_2R, we optimized PBMC labeling conditions by LEI121 in the presence of a panel of fluorescently labeled antibodies. Incubation of PBMCs with LEI121 followed by tandem photoclick chemistry led to increased mean fluorescence intensity (MFI) in each cell population (Figure 5B, middle panels). To determine the amount of specific CB_2R labeling, we performed the same experiment with a preincubation using an excess of CP55940, which resulted in decreased MFI in most cell populations (Figure 5B, middle panels). Quantification of this effect revealed a significant reduction in LEI121 labeling by CP55940 in $CD19^+$ B cells, $CD14^+$ monocytes, and $CD3^+$ T cells (Figure 5B, right panels). The highest specific fluorescent labeling was found in $CD19^+$ B-cells, followed by $CD14^+$ monocytes, whereas the signal was minimal in T-cells (Figure 5C, bar graph). These results indicate that CB_2R is expressed in only a selection of human immune cells. Using quantitative polymerase chain reaction (qPCR) as an orthogonal technique, we determined CB_2R mRNA levels in the immune cell populations studied, and found that CB_2R mRNA levels were also highest in B-cells, followed by monocytes and T-cells (Figure 5C, Northern blot).

DOI: 10.1021/jacs.7b11281
J. Am. Chem. Soc. XXXX, XXX, XXX−XXX

DISCUSSION

Recently, drug discovery research has focused on the development of selective CB_2R agonists for the treatment of tissue injury and inflammatory diseases that avoid inducing CB_1R-mediated psychoactive side effects. CB_2R knockout mice show enhanced pathology in various inflammatory disease models, including heart, liver, or kidney injury and inflammatory pain, thereby supporting the notion that CB_2R plays an essential role in these conditions. Despite compelling proof-of-concept data obtained in preclinical pain models, two CB_2R agonists lacked efficacy in phase 2 clinical trials.[12,21] The reasons for this nontranslatability are yet unclear. To validate the hypothesis that the CB_2R is a suitable therapeutic target for, for example, inflammatory pain, evidence is required that the receptor is expressed by relevant cell types in pain signaling pathways and, importantly, that investigational drugs fully engage with CB_2R in clinical trials. The absence of specific antibodies to detect CB_2R protein at the site of inflammation in patients and the lack of biomarkers to study their engagement is currently hampering the clinical development of CB_2R agonists. To address these challenges, new chemical tools are necessary to determine cellular CB_2R expression and to show receptor occupancy.

The work we have described allowed visualization of CB_2R expression and target engagement in human cells by photoaffinity-based protein profiling and fluorescence-activated cell sorting (FACS). The probe LEI121 was designed and synthesized to possess a diazirine as photoreactive group to capture CB_2R and an alkyne as ligation handle to enable visualization or isolation of the protein by conjugation to fluorophores or biotin, respectively. The study demonstrates that LEI121 is a potent CB_2R inverse agonist and selective over the closely related CB_1R. Using tandem photoclick chemistry, we noted that photoaffinity labeling of CB_2R-overexpressing CHO cell membranes resulted in visualization of two major species, corresponding to different glycosylated forms of the receptor. The labeling was dependent on UV-irradiation and copper-catalyzed conjugation of a fluorophore and could be prevented by preincubation with various, structurally diverse CB_2R ligands. In addition, we have shown that LEI121 labels endogenous CB_2R on HL-60 cells and primary human immune cells, which could be prevented by various, structurally diverse CB_2R ligands.

The development of LEI121 as a two-step photoaffinity probe provides new opportunities to study CB_2R biology. For example, LEI121 may serve as an alternative to the highly unselective CB_2R antibodies. Using LEI121, we have shown that B-cells exhibited the highest CB_2R levels, followed by monocytes, while minimal receptor levels were found in T-cells, which is in line with the CB_2R mRNA levels as determined in this study and as previously reported.[9] We envision that LEI121 may be used to profile CB_2R expression levels in PBMCs of patients suffering from inflammatory pain and/or other inflammatory diseases, such as rheumatoid arthritis, multiple sclerosis, and Crohn's disease. Next, isolation of CB_2R using the biotin-reporter and affinity enrichment from primary cells and tissues may facilitate the identification of potential protein interaction partners of the receptor. Additionally, the photoreactive probe may help in stabilizing CB_2R to facilitate crystallization studies of the protein.

Activity-based protein profiling (ABPP) using chemical probes with electrophilic warheads has been successfully applied to assess target engagement in living systems.[15,38,39,54] ABPP is, however, limited to protein families such as serine hydrolases, kinases, and proteases, which possess nucleophilic amino acids in their binding site that undergo covalent bond formation with the probe. The ABPP strategy has not been applied to the study of GPCRs due to a lack of mechanism-based rationale for probe design.

To the best of our knowledge, the present study represents the first successful application of two-step photoaffinity-based protein profiling to monitor endogenous GPCR expression and occupancy by small molecules in living human cells. Projecting forward, it is likely that strategically functionalized photoreactive probes can be used in preclinical animal models as well as in clinical settings to guide dose selection, thereby advancing translational drug discovery.

EXPERIMENTAL SECTION

Materials and General Remarks. All materials used are specified in the Supporting Information, as well as the synthetic procedures of LEI121, LEI120, and RO7239315. Molecules shown are drawn using Chemdraw, graphs and statistics were performed with Graphpad Prism 7, Bio-Rad Imagelab was used for gel analysis and quantification, online TOPO software was used to generate the snake plot in Figure 3, and FlowJo V10.1 (Miltenyi Biosciences) was used to analyze FACS data. In case of PBMC experiments, DIVA software from BD Biosciences was used for compensation of the fluorescence.

Molecular Modeling of LEI101 and LEI121. The X-ray structure of CB_1R with the stabilizing antagonist AM6538[42] (PDB entry 5TGZ) was used to build a CB_2R homology model for the docking of LEI101, as described in the Supporting Information.

Molecular Pharmacology of LEI121. CB_2R affinity, G protein activation, and β-arrestin recruitment were measured as reported previously.[12]

Radioligand Binding on LEI121 Pretreated Membranes from CB_2R-Overexpressing CHO Cells. [^{3}H]-CP55940 specific binding was determined using membranes of CB_2R-overexpressing CHO cells, pretreated with LEI121 (±UV) and THC in a washout experiment similar to previously reported procedures.[32] Specifications are provided in the Supporting Information.

Two-Step Covalent SDS-PAGE Visualization of LEI121 Labeling of CB_2R. CB_2R-CHO and WT CHO cell membrane aliquots were pretreated with competitor or vehicle, followed by incubation with LEI121. The samples were diluted, and irradiated using the Caprobox (λ = 350 nm). Control samples were denatured before UV-treatment, and No-UV controls were kept in the dark using aluminum foil until the ligation reaction was performed with Cy5-N_3 (**14**) for 1 h at room temperature. Samples without click mix received Milli-Q with the same % of DMSO. Finally, samples were denatured in 4× Laemmli sample buffer, and resolved by SDS-PAGE electrophoresis followed by in-gel fluorescence scanning using a Bio-Rad Chemidoc at the Cy5 channel. In-gel digestion was performed after coomassie staining according to published procedures.[55] Specifications are provided in the Supporting Information.

Two-Step Photoaffinity Enrichment and Mass Spectrometry-Based Proteomics of CB_2R. Cells were grown as specified in the Supporting Information. Live wild-type or CB_2R-overexpressing CHO cells were pretreated with DMSO or CP55940 and incubated with LEI121 (total volume: 3 mL).

The incubation solution was removed and replaced by 1.5 mL of fresh buffer, then the plates were immediately irradiated (except the No-UV control) for 5 min with Caprobox (λ = 350 nm), and the cells were harvested. The cells were lysed, and the membrane and cytosol fractions were separated. Ligation reaction was performed with biotin-N_3 (**15**). Protein was precipitated and washed to remove all click mix components, then denatured, reduced, and alkylated. The protein was added to avidin beads and incubated. The avidin beads were washed 4×, then digested overnight with trypsin containing buffer. Samples were quenched with formic acid (FA), and beads were removed using

DOI: 10.1021/jacs.7b11281
J. Am. Chem. Soc. XXXX, XXX, XXX−XXX

a biospin column. Peptides were added to C18 stagetips, washed, and then eluted. Peptides were concentrated using an Eppendorf SpeedVac and dissolved in LC/MS solution. Samples were measured using a NanoACQUITY UPLC System coupled to a SYNAPT G2-Si high definition mass spectrometer (Waters) and analyzed as specified in the Supporting Information, which contains also all other specifications of the pulldown procedure.

Two-Step Photoaffinity Visualization of Endogenous CB_2R by LEI121 Using FACS. All specifications of FACS experiments in HL-60 cells and freshly isolated human PBMCs are provided in the Supporting Information. Briefly, after extensive washing steps, the cells were counted and resuspended at 1×10^6 cells/mL, and 499 μL of cell suspension was added per sample. Pretreatment with competitor or DMSO was followed by treatment with LEI121 or DMSO. Unbound molecules were removed by centrifugation and the cells were resuspended in PBS (HL-60 cells), or antibody/isotype mixture or 1% BSA/PBS (PBMCs), followed by a short incubation time in case of the antibody stain. The cell suspensions then were irradiated with Caprobox (350 nm), then transferred to a V-bottom 96-well plate, and PBS was removed by centrifugation. Cells were fixed, washed, and blocked for 20 min with 1% BSA/PBS. The cells were pelleted and resuspended in ligation mixture containing AF647-N_3 (**16**). The cells were pelleted, washed, resuspended in 1% BSA/PBS, and analyzed with a Guava easyCyte HT (HL-60 cells) or a LSRII (PBMCs). Compensation of fluorescence was done using stained and unstained compensation beads using DIVA software (BD Biosciences), and further analysis was performed using FlowJo v10.1 (Miltenyi Biosciences).

Gene Expression Analysis of CB_2R mRNA in Human PBMC Populations. Peripheral blood mononuclear cells (PBMCs) were isolated from buffy coats, collected from multiple healthy human donors. Different cell types were separated by positive magnetic selection, and RNA was isolated and amplified by PCR. Amplicons were resolved on 2% agarose gels and analyzed using a G:Box gel documentation system (Syngene, Frederick, MD). Specifications are provided in the Supporting Information.

■ ASSOCIATED CONTENT

Supporting Information

The Supporting Information is available free of charge on the ACS Publications website at DOI: 10.1021/jacs.7b11281.

Experimental procedures, supporting figures, supporting tables, and compound characterization; mass spectrometry proteomics data have been deposited to the proteomeXchange Consortium via the PRIDE partner repository with the data set identifier PXD008460[56] (PDF)

■ AUTHOR INFORMATION

Corresponding Author

*m.van.der.stelt@chem.leidenuniv.nl

ORCID

Marjolein Soethoudt: 0000-0001-9220-3742
Hui Deng: 0000-0003-0899-4188
Sander I. van Kasteren: 0000-0003-3733-818X
Adriaan P. IJzerman: 0000-0002-1182-2259

Present Addresses

■Max Planck Institute for Plant Breeding Research, Carl-von-Linné-Weg 10, Köln 50829, Germany
○West China Hospital, West China Medical School, Sichuan University, Chengdu 610041, China

Notes

The authors declare no competing financial interest.

■ ACKNOWLEDGMENTS

M.S., L.H.H., and M.v.d.S. were supported by an ECHO-STIP grant from The Netherlands Organization for Scientific Research (NWO, grant 711.014.009). The Dutch Ministry of Education (Gravity Program "The Institute of Chemical Immunology") is acknowledged for financial support. We thank Caprotec for kindly providing the Caprobox. Hans van den Elst and Fons Lefeber are acknowledged for technical support. Dr. Richard van den Berg is acknowledged for critical feedback on the Supporting Information of this Article. Elisabeth Zirwes, Anja Osterwald, and Christoph Ullmer are acknowledged for the in vitro characterization of compounds **27**, **28**, **41**, and RO7239315.

■ REFERENCES

(1) Lagerstrom, M. C.; Schioth, H. B. *Nat. Rev. Drug Discovery* **2008**, *7*, 339.
(2) Katritch, V.; Cherezov, V.; Stevens, R. C. *Annu. Rev. Pharmacol. Toxicol.* **2013**, *53*, 531.
(3) Marinissen, M. J.; Gutkind, J. S. *Trends Pharmacol. Sci.* **2001**, *22*, 368.
(4) Munro, S.; Thomas, K. L.; Abu-Shaar, M. *Nature* **1993**, *365*, 61.
(5) Pacher, P.; Mechoulam, R. *Prog. Lipid Res.* **2011**, *50*, 193.
(6) Guindon, J.; Hohmann, A. G. *Br. J. Pharmacol.* **2008**, *153*, 319.
(7) Mackie, K. *Handb Exp Pharmacol* **2005**, *168*, 299.
(8) Mechoulam, R.; Hanus, L. O.; Pertwee, R.; Howlett, A. C. *Nat. Rev. Neurosci.* **2014**, *15*, 757.
(9) Galiegue, S.; Mary, S.; Marchand, J.; Dussossoy, D.; Carriere, D.; Carayon, P.; Bouaboula, M.; Shire, D.; Le Fur, G.; Casellas, P. *Eur. J. Biochem.* **1995**, *232*, 54.
(10) Han, S.; Thatte, J.; Buzard, D. J.; Jones, R. M. *J. Med. Chem.* **2013**, *56*, 8224.
(11) Mukhopadhyay, P.; Baggelaar, M.; Erdelyi, K.; Cao, Z.; Cinar, R.; Fezza, F.; Ignatowska-Janlowska, B.; Wilkerson, J.; van Gils, N.; Hansen, T.; Ruben, M.; Soethoudt, M.; Heitman, L.; Kunos, G.; Maccarrone, M.; Lichtman, A.; Pacher, P.; Van der Stelt, M. *Br. J. Pharmacol.* **2016**, *173*, 446.
(12) Soethoudt, M.; Grether, U.; Fingerle, J.; Grim, T. W.; Fezza, F.; de Petrocellis, L.; Ullmer, C.; Rothenhausler, B.; Perret, C.; van Gils, N.; Finlay, D.; MacDonald, C.; Chicca, A.; Gens, M. D.; Stuart, J.; de Vries, H.; Mastrangelo, N.; Xia, L.; Alachouzos, G.; Baggelaar, M. P.; Martella, A.; Mock, E. D.; Deng, H.; Heitman, L. H.; Connor, M.; Di Marzo, V.; Gertsch, J.; Lichtman, A. H.; Maccarrone, M.; Pacher, P.; Glass, M.; van der Stelt, M. *Nat. Commun.* **2017**, *8*, 13958.
(13) Horvath, B.; Magid, L.; Mukhopadhyay, P.; Batkai, S.; Rajesh, M.; Park, O.; Tanchian, G.; Gao, R. Y.; Goodfellow, C. E.; Glass, M.; Mechoulam, R.; Pacher, P. *Br. J. Pharmacol.* **2012**, *165*, 2462.
(14) Rajesh, M.; Pan, H.; Mukhopadhyay, P.; Batkai, S.; Osei-Hyiaman, D.; Hasko, G.; Liaudet, L.; Gao, B.; Pacher, P. *J. Leukocyte Biol.* **2007**, *82*, 1382.
(15) Simon, G. M.; Niphakis, M. J.; Cravatt, B. F. *Nat. Chem. Biol.* **2013**, *9*, 200.
(16) Tyler, D. S.; Vappiani, J.; Caneque, T.; Lam, E. Y. N.; Ward, A.; Gilan, O.; Chan, Y. C.; Hienzsch, A.; Rutkowska, A.; Werner, T.; Wagner, A. J.; Lugo, D.; Gregory, R.; Ramirez Molina, C.; Garton, N.; Wellaway, C. R.; Jackson, S.; MacPherson, L.; Figueiredo, M.; Stolzenburg, S.; Bell, C. C.; House, C.; Dawson, S. J.; Hawkins, E. D.; Drewes, G.; Prinjha, R. K.; Rodriguez, R.; Grandi, P.; Dawson, M. A. *Science* **2017**, *356*, 1397.
(17) Bunnage, M. E.; Chekler, E. L.; Jones, L. H. *Nat. Chem. Biol.* **2013**, *9*, 195.
(18) Cooper, A.; Singh, S.; Hook, S.; Tyndall, J. D. A.; Vernall, A. J. *Pharmacol. Rev.* **2017**, *69*, 316.
(19) Cecyre, B.; Thomas, S.; Ptito, M.; Casanova, C.; Bouchard, J. F. *Naunyn-Schmiedeberg's Arch. Pharmacol.* **2014**, *387*, 175.
(20) Marchalant, Y.; Brownjohn, P. W.; Bonnet, A.; Kleffmann, T.; Ashton, J. C. *J. Histochem. Cytochem.* **2014**, *62*, 395.

DOI: 10.1021/jacs.7b11281
J. Am. Chem. Soc. XXXX, XXX, XXX−XXX

(21) Ostenfeld, T.; Price, J.; Albanese, M.; Bullman, J.; Guillard, F.; Meyer, I.; Leeson, R.; Costantin, C.; Ziviani, L.; Nocini, P. F.; Milleri, S. *Clin J. Pain* **2011**, *27*, 668.
(22) Martin-Couce, L.; Martin-Fontecha, M.; Capolicchio, S.; Lopez-Rodriguez, M. L.; Ortega-Gutierrez, S. *J. Med. Chem.* **2011**, *54*, 5265.
(23) Yates, A. S.; Doughty, S. W.; Kendall, D. A.; Kellam, B. *Bioorg. Med. Chem. Lett.* **2005**, *15*, 3758.
(24) Petrov, R. R.; Ferrini, M. E.; Jaffar, Z.; Thompson, C. M.; Roberts, K.; Diaz, P. *Bioorg. Med. Chem. Lett.* **2011**, *21*, 5859.
(25) Martin-Couce, L.; Martin-Fontecha, M.; Palomares, O.; Mestre, L.; Cordomi, A.; Hernangomez, M.; Palma, S.; Pardo, L.; Guaza, C.; Lopez-Rodriguez, M. L.; Ortega-Gutierrez, S. *Angew. Chem., Int. Ed.* **2012**, *51*, 6896.
(26) Sexton, M.; Woodruff, G.; Horne, E. A.; Lin, Y. H.; Muccioli, G. G.; Bai, M.; Stern, E.; Bornhop, D. J.; Stella, N. *Chem. Biol.* **2011**, *18*, 563.
(27) Zhang, S.; Shao, P.; Bai, M. *Bioconjugate Chem.* **2013**, *24*, 1907.
(28) Wu, Z.; Shao, P.; Zhang, S.; Bai, M. *J. Biomed. Opt.* **2014**, *19*, 36006.
(29) Ling, X.; Zhang, S.; Shao, P.; Li, W.; Yang, L.; Ding, Y.; Xu, C.; Stella, N.; Bai, M. *Biomaterials* **2015**, *57*, 169.
(30) Zhang, S.; Jia, N.; Shao, P.; Tong, Q.; Xie, X. Q.; Bai, M. *Chem. Biol.* **2014**, *21*, 338.
(31) Geurink, P. P.; Prely, L. M.; van der Marel, G. A.; Bischoff, R.; Overkleeft, H. S. *Top. Curr. Chem.* **2011**, *324*, 85.
(32) Dixon, D. D.; Tius, M. A.; Thakur, G. A.; Zhou, H.; Bowman, A. L.; Shukla, V. G.; Peng, Y.; Makriyannis, A. *Bioorg. Med. Chem. Lett.* **2012**, *22*, 5322.
(33) Ogawa, G.; Tius, M. A.; Zhou, H.; Nikas, S. P.; Halikhedkar, A.; Mallipeddi, S.; Makriyannis, A. *J. Med. Chem.* **2015**, *58*, 3104.
(34) Gregory, K. J.; Velagaleti, R.; Thal, D. M.; Brady, R. M.; Christopoulos, A.; Conn, P. J.; Lapinsky, D. J. *ACS Chem. Biol.* **2016**, *11*, 1870.
(35) Grunbeck, A.; Sakmar, T. P. *Biochemistry* **2013**, *52*, 8625.
(36) Burgermeister, W.; Nassal, M.; Wieland, T.; Helmreich, E. J. M. *Biochim. Biophys. Acta, Biomembr.* **1983**, *729*, 219.
(37) Blex, C.; Michaelis, S.; Schrey, A. K.; Furkert, J.; Eichhorst, J.; Bartho, K.; Gyapon Quast, F.; Marais, A.; Hakelberg, M.; Gruber, U.; Niquet, S.; Popp, O.; Kroll, F.; Sefkow, M.; Schulein, R.; Dreger, M.; Koster, H. *ChemBioChem* **2017**, *18*, 1639.
(38) Niphakis, M. J.; Lum, K. M.; Cognetta, A. B., 3rd; Correia, B. E.; Ichu, T. A.; Olucha, J.; Brown, S. J.; Kundu, S.; Piscitelli, F.; Rosen, H.; Cravatt, B. F. *Cell* **2015**, *161*, 1668.
(39) Hulce, J. J.; Cognetta, A. B.; Niphakis, M. J.; Tully, S. E.; Cravatt, B. F. *Nat. Methods* **2013**, *10*, 259.
(40) Ong, S. E.; Schenone, M.; Margolin, A. A.; Li, X.; Do, K.; Doud, M. K.; Mani, D. R.; Kuai, L.; Wang, X.; Wood, J. L.; Tolliday, N. J.; Koehler, A. N.; Marcaurelle, L. A.; Golub, T. R.; Gould, R. J.; Schreiber, S. L.; Carr, S. A. *Proc. Natl. Acad. Sci. U. S. A.* **2009**, *106*, 4617.
(41) van der Stelt, M.; Cals, J.; Broeders-Josten, S.; Cottney, J.; van der Doelen, A. A.; Hermkens, M.; de Kimpe, V.; King, A.; Klomp, J.; Oosterom, J.; Pols-de Rooij, I.; de Roos, J.; van Tilborg, M.; Boyce, S.; Baker, J. *J. Med. Chem.* **2011**, *54*, 7350.
(42) Hua, T.; Vemuri, K.; Pu, M.; Qu, L.; Han, G. W.; Wu, Y.; Zhao, S.; Shui, W.; Li, S.; Korde, A.; Laprairie, R. B.; Stahl, E. L.; Ho, J. H.; Zvonok, N.; Zhou, H.; Kufareva, I.; Wu, B.; Zhao, Q.; Hanson, M. A.; Bohn, L. M.; Makriyannis, A.; Stevens, R. C.; Liu, Z. J. *Cell* **2016**, *167*, 750.
(43) Chouhan, G.; James, K. *Org. Lett.* **2013**, *15*, 1206.
(44) Worrell, B. T.; Malik, J. A.; Fokin, V. V. *Science* **2013**, *340*, 457.
(45) Himo, F.; Lovell, T.; Hilgraf, R.; Rostovtsev, V. V.; Noodleman, L.; Sharpless, K. B.; Fokin, V. V. *J. Am. Chem. Soc.* **2005**, *127*, 210.
(46) Luo, Y.; Blex, C.; Baessler, O.; Glinski, M.; Dreger, M.; Sefkow, M.; Koster, H. *Mol. Cell. Proteomics* **2009**, *8*, 2843.
(47) Soethoudt, M.; van Gils, N.; van der Stelt, M.; Heitman, L. H. *Methods Mol. Biol.* **2016**, *1412*, 103.
(48) Chang, L. C.; von Frijtag Drabbe Kunzel, J. K.; Mulder-Krieger, T.; Spanjersberg, R. F.; Roerink, S. F.; van den Hout, G.; Beukers, M. W.; Brussee, J.; Ijzerman, A. P. *J. Med. Chem.* **2005**, *48*, 2045.
(49) Cabral, G. A.; Griffin-Thomas, L. *Expert Rev. Mol. Med.* **2009**, *11*, 11.
(50) Filppula, S.; Yaddanapudi, S.; Mercier, R.; Xu, W.; Pavlopoulos, S.; Makriyannis, A. *J. Pept. Res.* **2004**, *64*, 225.
(51) Derocq, J. M.; Jbilo, O.; Bouaboula, M.; Segui, M.; Clere, C.; Casellas, P. *J. Biol. Chem.* **2000**, *275*, 15621.
(52) Kleyer, J.; Nicolussi, S.; Taylor, P.; Simonelli, D.; Furger, E.; Anderle, P.; Gertsch, J. *Biochem. Pharmacol.* **2012**, *83*, 1393.
(53) *Bull. World Health Organ* **1984**, *62*, 809.
(54) van Esbroeck, A. C. M.; Janssen, A. P. A.; Cognetta, A. B., 3rd; Ogasawara, D.; Shpak, G.; van der Kroeg, M.; Kantae, V.; Baggelaar, M. P.; de Vrij, F. M. S.; Deng, H.; Allara, M.; Fezza, F.; Lin, Z.; van der Wel, T.; Soethoudt, M.; Mock, E. D.; den Dulk, H.; Baak, I. L.; Florea, B. I.; Hendriks, G.; De Petrocellis, L.; Overkleeft, H. S.; Hankemeier, T.; De Zeeuw, C. I.; Di Marzo, V.; Maccarrone, M.; Cravatt, B. F.; Kushner, S. A.; van der Stelt, M. *Science* **2017**, *356*, 1084.
(55) Shevchenko, A.; Tomas, H.; Havlis, J.; Olsen, J. V.; Mann, M. *Nat. Protoc.* **2006**, *1*, 2856.
(56) Vizcaino, J. A.; Csordas, A.; del-Toro, N.; Dianes, J. A.; Griss, J.; Lavidas, I.; Mayer, G.; Perez-Riverol, Y.; Reisinger, F.; Ternent, T.; Xu, Q. W.; Wang, R.; Hermjakob, H. *Nucleic Acids Res.* **2016**, *44*, D447.

DOI: 10.1021/jacs.7b11281
J. Am. Chem. Soc. XXXX, XXX, XXX−XXX